Transactions of the Korean Nuclear Society Spring Meeting
Jeju, Korea, May 18-19, 2023

2D FDM Structural Analysis Model for Cr-coated ATF cladding: Development and implementation into fuel analysis code

Hyuntaek Rho, Youho Lee*
Seoul National University, 1 Gwanak-ro, Gwanak-gu, Seoul 08826, Korea

**Corresponding author: leeyouho@snu.ac.kr*

1. Introduction

The need to improve the safety, reliability and efficiency of nuclear reactors has led to the development of fuel cladding structural analysis codes. Nuclear fuel cladding is essential to prevent the release of radioactive materials from fuel pellets into the cooling water. Therefore, it is important to generate code that can accurately predict how a cladding material will behave in a variety of operating environments.

In addition, with the development of ATF technologies such as coated cladding and SiC cladding, the need for accurate and reliable structural analysis codes has increased. These technologies offer the potential for improved safety, performance, and efficiency, but require advanced modeling techniques to fully understand their behavior under various operating conditions.

In response to these challenges, we have been working to develop advanced structural analysis codes that can accurately predict the behavior of fuel cladding materials. This includes the development of two-dimensional Finite Difference Method (FDM) structural analysis models for ATF cladding structures, which can improve computational efficiency and reduce modeling complexity.

The US NRC previously developed a nuclear fuel code known as FRAPCON, which utilizes a 1.5-dimensional structural analysis model that does not account for axial interactions. Axial interactions refer to the complex interactions that occur between different sections of the fuel rod in the axial direction, such as thermal expansion, fission gas release, and pellet-cladding mechanical interaction. By neglecting axial interactions, the FRAPCON model may not accurately predict the behavior of the fuel rod under certain conditions, which can affect its safety and performance. To address this issue, the present study has developed a new code that utilizes a two-dimensional structural analysis model with axial symmetry. This approach enhances calculation speed while maintaining high accuracy, as demonstrated through comparison with a Finite Element Analysis (FEA) code.

In a prior research [1], an analytical model named FRACAS-CT was created to compute the mechanical behavior of multilayered ATF cladding in steady-state in-reactor conditions. This model enabled the calculation of stress distribution in double cladding by employing the thick-walled cylinder assumption. In the present study, a more advanced model was utilized that employs the FDM without the use of the thick-walled cylinder assumption.

In this study, we concentrate on the structural analysis of Cr-coated cladding among ATFs. The analysis considers large deformations and plasticity, which were not fully considered in previous studies of SiC cladding [2].

2. Code Development

A 2D FDM structural analysis code is appropriate for nuclear fuel cladding structures because the cladding has a long axial length compared to its radial length. This makes it easier to represent the cladding in a two-dimensional analysis rather than a three-dimensional one, which can significantly reduce computational costs.

In addition, the axial symmetry of the cladding structure allows for simplifications in the analysis process. The FDM method can easily incorporate these symmetries to develop an efficient and accurate analysis model. By using a 2D FDM code, one can obtain a more accurate and efficient analysis of the cladding behavior, as it can consider the axial interactions and provide insight into the stress and strain distribution throughout the cladding.

Overall, a 2D FDM structural analysis code can be an effective tool for analyzing the behavior of nuclear fuel cladding structures, as it offers a good balance between computational efficiency and accuracy.

2.1 Mechanical Equations

The 2D FDM structural analysis code assumes the mechanical behavior of an axisymmetric cladding. The equilibrium equations for an axisymmetric cylinder can be expressed as follows:

$$\frac{\partial \sigma_{rr}}{\partial r} + \frac{\partial \tau_{rz}}{\partial z} + \frac{\sigma_{rr} - \sigma_{\theta\theta}}{r} = 0 \tag{1}$$

$$\frac{\partial \sigma_{zz}}{\partial z} + \frac{\partial \tau_{rz}}{\partial r} + \frac{\tau_{zr}}{r} = 0 \tag{2}$$

Here, σ_{rr}, $\sigma_{\theta\theta}$, σ_{zz}, and τ_{rz} represent the radial, hoop, axial, and shear stresses, respectively.

Considering the large deformation, the stress and strain of the current time step are defined by adding the difference to the value of the previous time step. In the equation below, the current time step is represented by n+1, and the previous time step is represented by n.

$$\sigma_{n+1} = \sigma_n + \Delta\sigma \quad (3)$$

$$\epsilon_{n+1} = \epsilon_n + \Delta\epsilon \quad (4)$$

The amount of change in stress is defined by the following equation.

$$\Delta\sigma = C^{elastic} : [\Delta\epsilon - \Delta\epsilon^{creep} - \Delta\epsilon^{plastic} - \Delta\epsilon^{thermal}] \quad (5)$$

The formula involves four variables: $\Delta\epsilon$, $\Delta\epsilon^{creep}$, $\Delta\epsilon^{plastic}$, and $\Delta\epsilon^{thermal}$, which represent the total strain change, the strain change due to creep, the strain change due to plastic deformation, and the thermal strain change, respectively.

Constitutive equations (Hooke's Law) can be expressed as follows:

$$\epsilon_{rr} = \frac{\sigma_{rr}}{E_{rr}} - \frac{\nu_{\theta r}\sigma_{\theta\theta}}{E_{\theta\theta}} - \frac{\nu_{zr}\sigma_{zz}}{E_{zz}} + \alpha_{rr}\Delta T + Ext_{rr} \quad (6)$$

$$\epsilon_{\theta\theta} = \frac{\sigma_{\theta\theta}}{E_{\theta\theta}} - \frac{\nu_{z\theta}\sigma_{zz}}{E_{zz}} - \frac{\nu_{r\theta}\sigma_{rr}}{E_{rr}} + \alpha_{\theta\theta}\Delta T + Ext_{\theta\theta} \quad (7)$$

$$\epsilon_{zz} = \frac{\sigma_{zz}}{E_{zz}} - \frac{\nu_{rz}\sigma_{rr}}{E_{rr}} - \frac{\nu_{\theta z}\sigma_{\theta\theta}}{E_{\theta\theta}} + \alpha_{zz}\Delta T + Ext_{zz} \quad (8)$$

$$\gamma_{rz} = \frac{\tau_{rz}}{G} \quad (9)$$

Here, α represents the coefficient of thermal expansion, ΔT represents the temperature difference from the strain-free reference temperature (T_{ref}), and Ext represents the viscoplastic strain, such as plastic strain and creep strain. E, ν, and G are Young's modulus, Poisson's ratio, and shear modulus, respectively.

The kinematic relation between displacement and strain is as follows:

$$\Delta\epsilon_{rr} = \frac{\partial \Delta u_r}{\partial r} \quad (10)$$

$$\Delta\epsilon_{\theta\theta} = \frac{\Delta u_r}{r} \quad (11)$$

$$\Delta\epsilon_{zz} = \frac{\partial \Delta u_z}{\partial z} \quad (12)$$

$$\Delta\gamma_{rz} = \frac{\partial \Delta u_r}{\partial z} + \frac{\partial \Delta u_z}{\partial r} \quad (13)$$

Here, $\Delta\epsilon_{rr}$, $\Delta\epsilon_{\theta\theta}$, $\Delta\epsilon_{zz}$, and $\Delta\gamma_{rz}$ denote the radial, hoop, axial, and shear strain differences, respectively, while Δu_r and Δu_z represent radial and axial displacement differences, respectively.

The relationship between effective plastic strain and plastic strain in each direction is as follows:

$$d\epsilon^p = \frac{\sqrt{2}}{3}[(d\epsilon_r^p - d\epsilon_\theta^p)^2 + (d\epsilon_\theta^p - d\epsilon_z^p)^2 + (d\epsilon_z^p - d\epsilon_r^p)^2]^{1/2} \quad (14)$$

The Prandtl-Reuss flow equations are as follows:

$$d\epsilon_i^p = \frac{3}{2}\frac{d\epsilon^p}{\sigma_e}[\sigma_i - \frac{1}{3}(\sigma_r + \sigma_\theta + \sigma_z)], i = r, \theta, z \quad (15)$$

The calculation of the plastic strain increment for each direction is performed by the following process.

1) Value of $d\epsilon_\theta{}^p$, $d\epsilon_r{}^p$, and $d\epsilon_z{}^p$ are assumed. Then, $d\epsilon^p$ is computed from Eq. (14) and the effective stress is obtained from the stress-strain curve at the value of $d\epsilon^p$.
2) Conduct structural analysis based on the plastic strain increments assumed in 1), and save the calculated stress in each direction.
3) Eq. (15) is used to calculate the plastic strain increment for each new direction. The value calculated in 1) is used for the effective stress, and the value calculated in 2) is used for the stress in each direction.
4) If the newly calculated plastic strain increment for each direction has a large difference from the existing value, use the corresponding value as the source of 1) again, and proceed with the iterative calculation.
5) When the difference between the old value and the newly calculated value becomes sufficiently small, the iterative calculation is stopped.

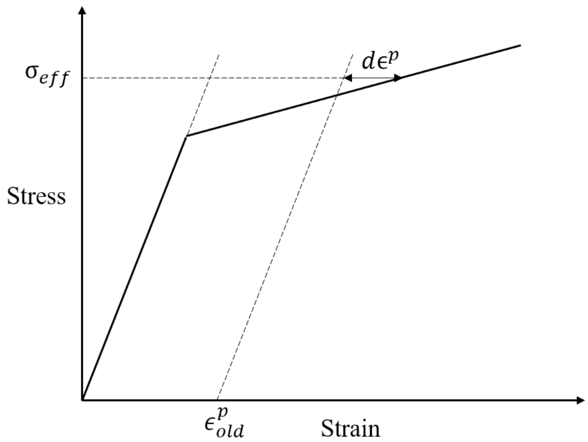

Fig. 1. Schematic diagram for calculating plastic strain using stress-strain curve

2.2 Boundary Conditions

When a thin-walled cylindrical shell such as nuclear fuel cladding is subjected to internal pressure and external pressure, the following mechanical boundary conditions can be considered:

1) Axial stress: The axial stress in the cladding is caused by the internal and external pressure and is given by:

$$\sigma_z = \frac{P_i r_i^2 - P_o r_o^2}{r_o^2 - r_i^2} \tag{16}$$

where P_i and P_o are the internal and external pressure, respectively, r_i and r_o are the inner and outer radii of the cladding, and σ_z is the axial stress.

2) Radial stress: At the inner surface of the cladding, the radial stress (σ_r) must be equal to the internal pressure (P_i). At the outer surface of the cladding, the radial stress (σ_r) must be equal to the external pressure (P_o)

3) Shear stress: The shear stress at the inner and outer surfaces can be considered to be zero. This is because the shear stress is a result of the deformation of the material in the tangential direction, which is constrained by the adjacent material. However, at a free surface, there is no adjacent material to constrain the deformation, and so the shear stress is zero.

4) Axial displacement: There is no axial deformation at the bottom.

Fig. 2. shows a schematic diagram of the boundary conditions and 2D FDM meshes utilized in the analysis.

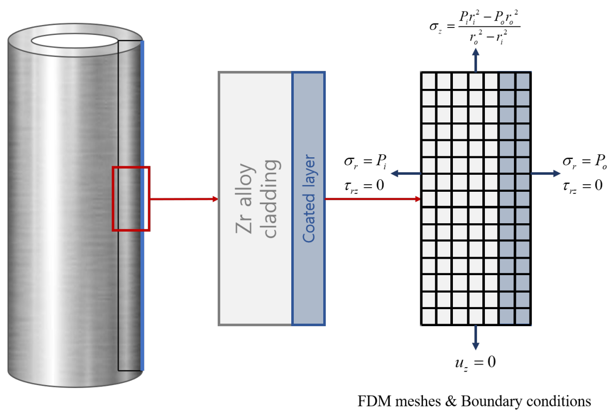

Fig. 2. Schematic diagram of the boundary conditions and finite difference method (FDM) meshes used in the analysis.

2.3. Boundary condition modification method for PCMI simulation

In analyzing the behavior of nuclear fuel cladding, if contact occurs between the pellet and the cladding, two assumptions are made.

1) The first assumption is that the radial displacement of the fuel is transferred to the cladding after contact occurs, based on the principle of radial continuity. This is expressed mathematically as shown in equation (17).

$$u_r^{clad} = u_r^{fuel} - \delta \tag{17}$$

Where u_r^{clad} represents the radial displacement of the cladding, u_r^{fuel} represents the radial displacement of the fuel, and δ represents the as-fabricated fuel-cladding gap size.

2) The second assumption is that no slippage occurs between the fuel and the cladding in the axial direction after contact has occurred. This means that any additional strains that develop in the fuel after contact are transferred to the cladding. Mathematically, this is expressed in equation (18).

$$\varepsilon_z^{clad} - \varepsilon_{z,o}^{clad} = \varepsilon_z^{fuel} - \varepsilon_{z,o}^{fuel} \tag{18}$$

Where ε_z^{clad} and ε_z^{fuel} are the current axial strain of the cladding and fuel, respectively, and $\varepsilon_{z,o}^{clad}$ and $\varepsilon_{z,o}^{fuel}$ are axial strains of the cladding and fuel before the gap is closed respectively.

Fig. 3. shows a schematic diagram of the boundary conditions changes due to PCMI.

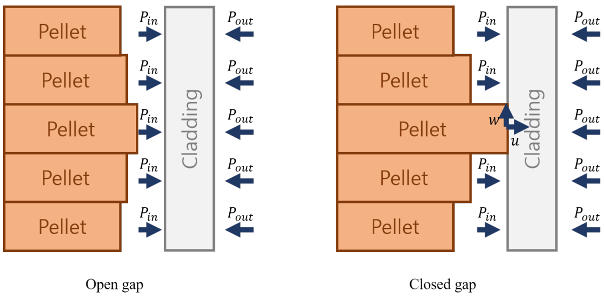

Fig. 3. Changes in boundary conditions due to contact between a part of the cladding and pellets

3. Code Verification

To verify the developed FDM model, the stress calculation results were compared with those obtained layer from ANSYS code. A pressurized tube with a coated was simulated with an inner radius of 10 mm, outer radius of 16 mm, and coating layer thickness of 1 mm. The Young's modulus and Poisson's ratio of the matrix were 200 GPa and 0.3, respectively, while those of the coating layer were 100 GPa and 0.2, respectively. The thermal stress was neglected in this analysis. The tube was subjected to an internal pressure of 125 MPa and an external pressure of 0.1 MPa, and the other mechanical boundary conditions were as discussed in Section 2.2. During the simulation, the yield stress and tangent modulus of the matrix were determined to be 300 MPa and 200 MPa, respectively.

Table I: Material properties of the matrix and coated layer in the simulation.

	Matrix	Coated layer
Radial position	10~15mm	15~16mm
Young's modulus	200 GPa	100 GPa
Poisson's ratio	0.3	0.2

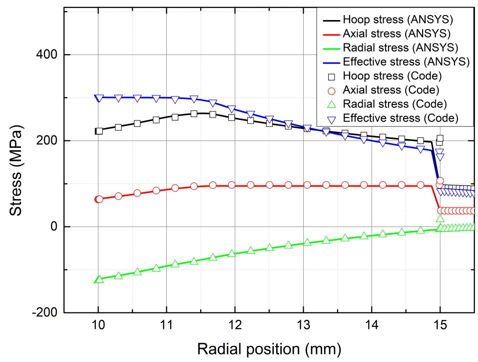

Fig. 4. Comparison of stress calculation results (multi-layer & plasticity) between ANSYS and developed code: ANSYS (solid line) and developed code (open symbol)

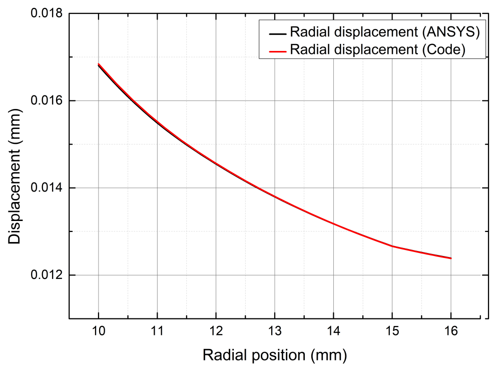

Fig. 5. Comparison of displacement calculation results (multi-layer & plasticity) between ANSYS and developed code: ANSYS (solid line) and developed code (open symbol)

Fig. 4. depicts the stress calculation results obtained from the developed code and ANSYS, indicating excellent agreement between the two methods. Additionally, Fig. 5. displays the radial displacement as a function of radial position, showing high accuracy in the simulation results.

The present code has demonstrated a high level of accuracy in matching calculation results, even when plasticity is considered.

4. Code Results

Simulation was performed using a previously developed code in the actual geometry and environment of coated Zr cladding. The cladding structure consisted of a Zr inner radius of 4.18 mm, an outer radius of 4.75 mm, and a height of 3.66 m, with a 16 μm thick Cr coating layer. The Young's modulus and Poisson's ratio of Zr were 99 MPa and 0.35, respectively, while those of Cr were 279 GPa and 0.21, respectively. The geometry of the cladding is summarized in Table 2. The simulation conditions involved an internal pressure of 7 MPa and an external pressure of 15.5 MPa.

Table II: Material properties of the Zr and Cr layer in the simulation.

	Zr layer	Cr layer (Coating)
Radial position	4.18~4.75 mm	Thickness: 16μm
Young's modulus	99 GPa	279 GPa
Poisson's ratio	0.35	0.21

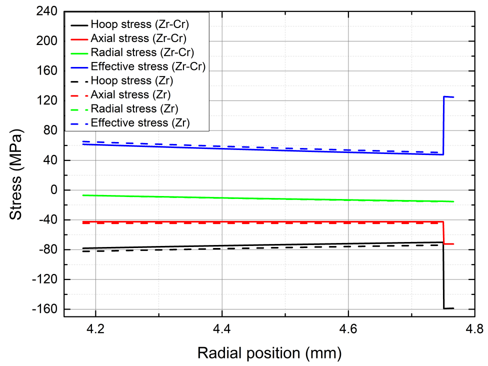

Fig. 6. Comparison of stress calculation results between Zr-Cr (solid line) and Zr (dotted line) cladding. r_{in} =4.18 mm, r_{out} =4.75 mm, Coating thickness= 16 μm, P_{in} = 7 MPa, P_{out} =15.5 MPa

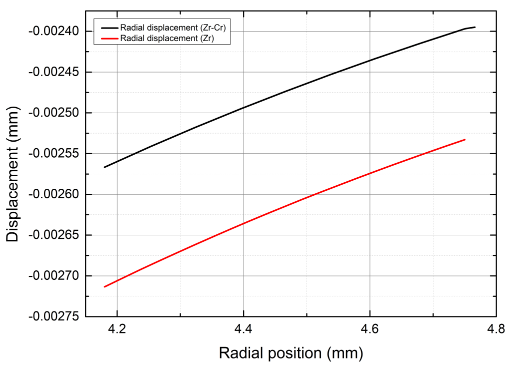

Fig. 7. Comparison of displacement calculation results between Zr-Cr (solid line) and Zr (dotted line) cladding. r_{in} =4.18 mm, r_{out} =4.75 mm, Coating thickness= 16 μm,

P_{in} = 7 MPa, P_{out} =15.5 MPa

Upon analyzing Fig. 6. and Fig. 7., it was observed that in Zr-Cr cladding with a coating layer, the stress distribution of the matrix was slightly alleviated compared to the single-layer Zr cladding. Furthermore, a significant reduction in radial displacement was confirmed.

This phenomenon can be attributed to two factors. Firstly, the Young's modulus of the coating layer is generally higher than that of the matrix. Secondly, the overall thickness of the cladding is increased by the coating layer.

5. Conclusion

In conclusion, a 2D FDM code was successfully developed for the analysis of ATF structures, with a particular focus on coated cladding. The developed code exhibited a fast calculation speed and provided highly accurate stress and strain calculation results when compared with 3D FEA calculations. Furthermore, the analysis results were consistent even when plasticity and large deformations, including creep, were considered. However, it is important to note that the developed code is limited by its assumption of axisymmetry and cannot be applied in cases where local ballooning or burst of cladding occurs. Therefore, it may be necessary to develop a 3D FDM model or link the developed code with a local FEA model to address this limitation. Overall, this study provides a valuable contribution to the development of ATF structural analysis codes and serves as a foundation for further research in this area.

ACKNOWLEDGEMENT

This work was supported by the Nuclear Safety Research Program through the Korea Foundation of Nuclear Safety (KoFONS) using the financial resource granted by the Nuclear Safety and Security Commission (NSSC) of the Republic of Korea [2101051 (50%)] and Korea Institute of Energy Technology Evaluation and Planning (KETEP) grant funded by the Korea government (MOTIE) (No. 20224B10200100, Development of Commercialization Technology for Enhanced Accident Tolerant Fuel) (50%).

REFERENCES

[1] D. Kim, H. Kim, C. Shin & H. Kim, Development of FRACAS-CT module with FRAPCON4.0P01 for simulation of mechanical behaviors for accident-tolerant fuel cladding in a reactor, Journal of Nuclear Science and Technology, Vol.56:8, 671-683, 2019

[2] H. Rho, Y. Lee, Development of a 2D axisymmetric SiC cladding mechanical model and its applications for steady-state and LBLOCA analysis. Journal of Nuclear Materials, Vol.558, 153311, 2022.